

## Scientific Article

# Treatment Time Optimization in Single Fraction Stereotactic Ablative Radiation Therapy: A 10-Year Institutional Experience



Mathieu Gaudreault, PhD,<sup>a,b,\*</sup> Adam Yeo, PhD,<sup>a,b</sup> Tomas Kron, PhD,<sup>a,b,c</sup>  
Gerard G. Hanna, PhD,<sup>b,d</sup> Shankar Siva, PhD,<sup>b,d</sup> and Nicholas Hardcastle, PhD<sup>a,b,c</sup>

<sup>a</sup>Department of Physical Sciences, Peter MacCallum Cancer Centre, Melbourne, Victoria, Australia; <sup>b</sup>Sir Peter MacCallum Department of Oncology, the University of Melbourne, Australia; <sup>c</sup>Centre for Medical Radiation Physics, University of Wollongong, New South Wales, Australia; <sup>d</sup>Division of Radiation Oncology, Peter MacCallum Cancer Centre, Melbourne, Victoria, Australia

Received March 18, 2021; accepted September 30, 2021

## Abstract

**Purpose:** Stereotactic ablative radiation therapy (SABR) delivered in a single fraction (SF) can be considered to have higher uncertainty given that the error probability is concentrated in a single session. This study aims to report the variation in technology and technique used and its effect on intrafraction motion based on a 10 years of experience in SF SABR.

**Methods and Materials:** Records of patients receiving SF SABR delivered at our institution between 2010 and 2019 were included. Treatment parameters were extracted from the patient management database by using an in-house script. Treatment time was defined as the time difference between the first image acquisition to the last beam off of a single session. The intrafraction variation was measured from the 3-dimensional couch displacement measured after the first cone beam computed tomography (CBCT) acquired during a treatment.

**Results:** The number of SF SABR increased continuously from 2010 to 2019 and were mainly lung treatments. Treatment time was minimized by using volumetric modulated arc therapy, flattening filter-free dose rate, and coplanar field ( $24 \pm 9$  min). Treatment time increased as the number of CBCTs per session increased. The most common scenario involved both 2 and 3 CBCTs per session. On the average, a CBCT acquisition added 6 minutes to the treatment time. All treatments considered, the average intrafraction variation was  $1.7 \pm 1.6$  mm.

**Conclusions:** SF SABR usage increased with time in our institution. The intrafraction motion was acceptable and therefore a single fraction is an efficacious treatment option when considering SABR.

© 2021 The Author(s). Published by Elsevier Inc. on behalf of American Society for Radiation Oncology. This is an open access article under the CC BY-NC-ND license (<http://creativecommons.org/licenses/by-nc-nd/4.0/>).

## Introduction

Stereotactic ablative radiation therapy (SABR) is characterized by a large dose per fraction and high biological effect, a small number of fractions (typically 1-5) and a specialized planning, delivery and QA.<sup>1,2</sup> SABR is more commonly applied to primary tumors or metastases in the lung, spine, prostate, liver, and oligometastatic tumors.<sup>3-9</sup>

Sources of support: This research was partially funded by Varian Medical Systems and by the Peter MacCallum Cancer Centre Foundation. Shankar Siva is supported by the Victorian Cancer Council Colebatch Fellowship.

Disclosures: none.

Research data are stored in an institutional repository and will be shared upon request to the corresponding author.

\*Corresponding author: Mathieu Gaudreault, PhD; E-mail: [mathieu.gaudreault@petermac.org](mailto:mathieu.gaudreault@petermac.org)

<https://doi.org/10.1016/j.adro.2021.100829>

2452-1094/© 2021 The Author(s). Published by Elsevier Inc. on behalf of American Society for Radiation Oncology. This is an open access article under the CC BY-NC-ND license (<http://creativecommons.org/licenses/by-nc-nd/4.0/>).

The safety of SABR relies on the minimization of the volume of critical organs receiving a high dose. This necessitates tight geometric margins, enabled by daily image guidance based on soft-tissue imaging and or implanted fiducial markers. Multifractionation treatment reduces the overall risk of intrafraction errors due to patient movement. Furthermore, the safety of SABR with respect to critical organ doses can be maximized by increasing the number of fractions. Fractionation exploits tissue repair between fractions and can also vary the location of maximum doses as critical organs deform relative to the tumor. Lastly, the risk of dosimetric error due to interplay between tumors moving with respiration and multileaf collimator motion in modulated treatments is maximized in single fraction treatments.<sup>10</sup> For all these reasons, single fraction (SF) SABR may be considered as a high-risk treatment.

SF SABR is attractive in a resource limited environment,<sup>11,12</sup> and is more convenient for the patient, in particular with increased number of metastases treated per patient.<sup>3</sup> SF SABR has been demonstrated to be effective and safe, with similar local control rates and toxicities compared with a multifractionation regime for lung,<sup>13-15</sup> oligometastasis to lung and bone,<sup>16</sup> spine,<sup>17,18</sup> and kidney.<sup>19,20</sup> The dosimetric accuracy of SF SABR however can be reduced through positional shifts of the tumor during treatment, and potentially by interplay between multileaf collimator motion and respiratory/cardiac motion.<sup>10,21,22</sup> Both of these are affected by treatment time.

In the present work, we evaluate 10 years of SF SABR treatments to determine treatment planning and delivery factors that affect treatment delivery time. We look at the relationship between treatment time and delivery technique including arc or static beams, noncoplanar beams, modulation, and use of flattening filter free (FFF) beams. We further evaluate patient intrafraction motion during SF SABR, to determine whether prolonged treatment delivery time is correlated with increased intrafraction motion.

## Methods and Materials

All single fraction SABR treatments from 2010 to 2019 treated across 5 campuses in our network were considered for inclusion. Data was extracted from the Mosaik SQL database (Mosaik, version 2.64, Elekta, CA) by using in-house script in Python. All treatments were delivered on either Varian Clinac iX or TrueBeam machine (Varian Medical Systems, Palo Alto, CA). Noncoplanar treatments were defined as those with at least one treatment field from a couch angle different from 0 degrees. All SF SABR treatments were delivered by using a 3 degrees of freedom couch, with the exception of those in which the ExacTrac IGRT system (BrainLab AG, Felkirchen, Germany) was used for image guidance.

According to our SABR protocol, all patients were treated in arms up position per default. If the patient is in pain at simulation session, we will prescribe pain medication for treatment, and in rare instances treat with the contralateral or both arms down. Furthermore, patients were routinely given 1 mg of lorazepam unless contraindicated, which is designed to be a mild sedative and may assist the stability of this position during treatment. Patients were immobilized using the Elekta BodyFix system (Elekta, Stockholm, Sweden). For tumors subject to respiratory motion in the lung and upper abdomen, the vacuum drape was used to limit respiratory motion.<sup>23</sup> Motion management for tumors that moved with respiration was in general internal target volume derived from the respiratory excursion of the tumor from a respiratory phase binned 4-dimensional CT acquired for treatment planning. In <10 cases, exhale phase gating was used.

Target locations were classified into 6 categories based on keywords found under the site name tag in the database, namely lung (lung), bone (bone), vertebra (vert), abdominal and pelvic node (node), kidney (kidney), and soft tissues (soft).

Treatment time was defined as the time difference between first image acquisition (kV or CBCT) to the last field beam-off time. Cases where 2 sites were treated in the same session were considered as 2 different treatments. Cases where treatment was interrupted during beam on and continued later due to system malfunction or patient discomfort were considered as one treatment. The overall treatment time of the 2 sessions was adjusted accordingly by removing the setup time. The modulation factor (MF) was calculated as the total monitor units normalized by the prescription dose in cGy.

The number of cone beam CTs (CBCT) acquired during a session was extracted. When required by a clinical trial protocol, when treatment time exceeded approximately 10 minutes, or at clinician discretion, a midtreatment CBCT (MID CBCT) was acquired to correct for intrafraction positioning variation during the treatment. MID CBCT was defined as the first CBCT acquired with shifts recorded in the database after some dose had been delivered to the patient. For some fractions, the shift was not recorded in the patient management system, and these were not included in the analysis. According to our protocol, CBCT acquisition was repeated if the translational shift was >2 mm in any direction for verification purposes. The right beam-on sequence for field and CBCT was not correctly recorded in the Mosaik database in some cases due to system failure. In these cases, identification of the mid treatment CBCT was performed using comments in the Mosaik imaging tab, which is in general carefully but manually populated. As a result, some MID CBCTs may have been missed but the number shown in this study represent a fairly good estimate. In some cases, a CBCT post treatment was acquired (POST CBCT) for research or trial purposes. POST CBCT was not included

in the calculation of treatment time and in the number of CBCTs per session. Intrafraction positioning variation was measured from the 3-dimensional couch shift measured after MID CBCT acquisition. Correlations between the intrafraction correction and either the total treatment time, or the time to MID CBCT, defined as the time difference between MID CBCT acquisition and the first pre-treatment image acquisition, were reported.

The ExacTrac IGRT system was used during SF SABR on one treatment unit for vertebra and bone sites. In these treatments, a couch correction was applied before each treatment field. These corrections were not recorded in the Mosaiq database and thus these treatments were excluded from the determination of the intrafraction correction but not in treatment time evaluation.

A Student *t* test was performed to establish the statistical significance of mean difference and the resulting *P* value was reported. Results were reported in terms of mean ± standard deviation to reflect skewed distribution. Correlations were reported by using the Spearman’s rank correlation coefficient ( $\rho$ ) and its associated *P* value.

## Results

### Overview of SF SABR

There were 1072 single fraction SABR treatments (334 coplanar/738 noncoplanar) between 2010 and 2019 at our institution. The time evolution of the number of SF SABR treatments is shown in Figure 1a. SF SABR treatments increased through years, from 9 treatments in 2010 to 221 treatments in 2019. FFF dose rate was commissioned in 2014. Lung was the most common treated site (49% of all SF treatments) as shown in Figure 1b. Other sites treated with SF SABR involved bone (25%), vertebra (11%), node (7%), kidney (7%), and soft tissues (1%). Prescription dose from 18 Gy to 28 Gy were used in SF SABR.

The treatment techniques used for SF SABR at our institution were 58% 3-dimensional conformal radiation therapy (3DCRT), 20% volumetric modulated arc therapy (VMAT), 14% dynamic conformal arc therapy (DCAT), and 8% intensity modulated radiation therapy (IMRT).

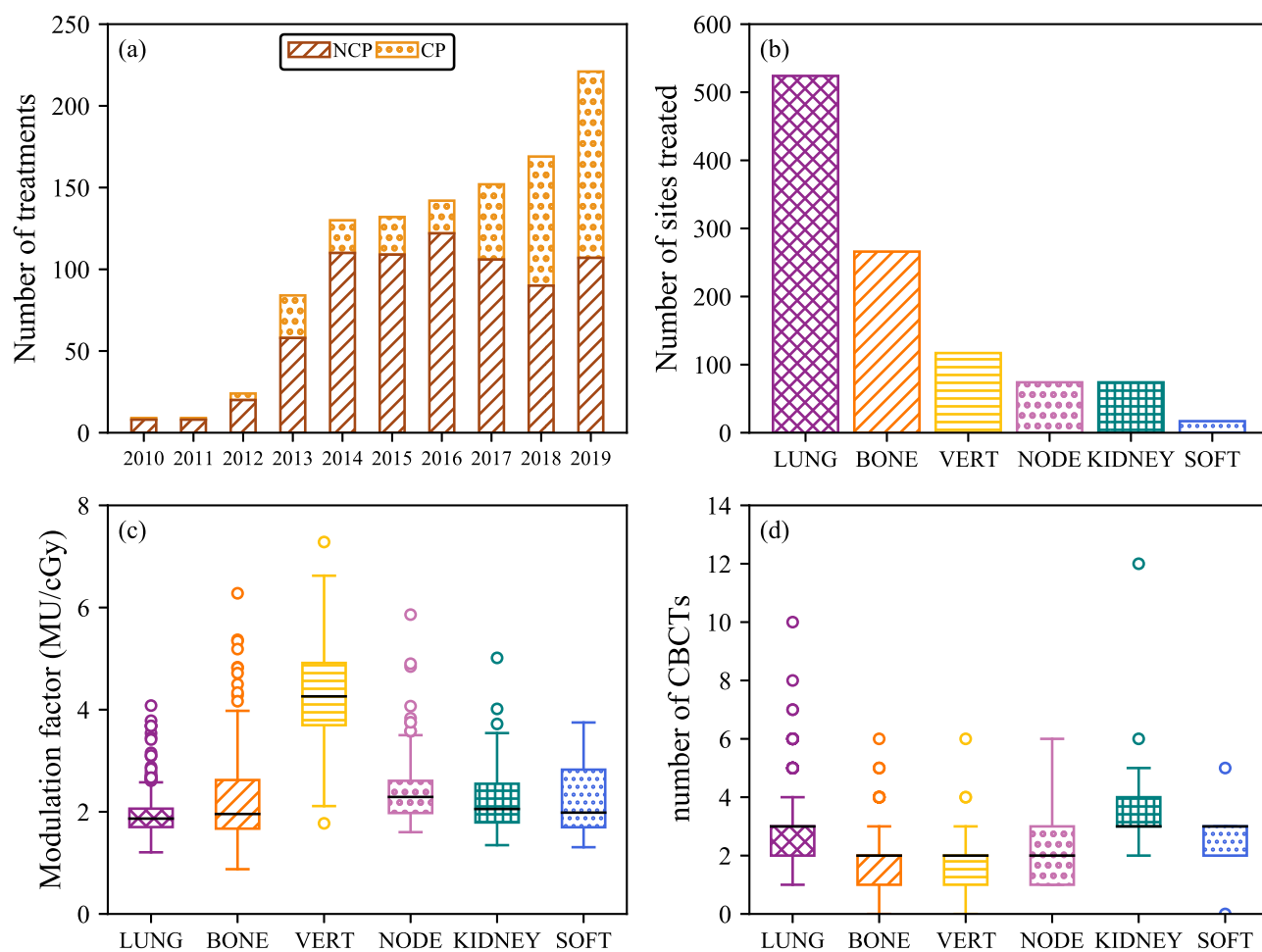


**Figure 1** (a) Time evolution of the number of single fraction stereotactic ablative radiation therapy treatments. Number of coplanar (CP) and noncoplanar (NCP) treatments is shown. (b) Number of sites treated in single fraction stereotactic ablative radiation therapy. (c) Modulation factor (MU/cGy) per site. (d) Number of cone beam computed tomographies acquired during a session per site.

3DCRT was the most frequent for lung sites (77% of all techniques), kidney sites (57%), bone sites (52%), and node sites (34%), and VMAT was the most used in vertebra sites (50%) and in soft tissue sites (47%).

Figure 1c shows the distribution of MF per site. MF was higher in vertebral treatments compared with all other sites mostly because 98% of vertebra treatment were delivered using VMAT or IMRT (MF in vertebra =  $4.3 \pm 1.0$  MU/cGy,  $P$  value  $< 10^{-10}$  compared with all other sites). The lowest MF was in lung sites (MF in lung =  $1.9 \pm 0.4$  MU/cGy,  $P$  value  $< 10^{-3}$  compared with all other sites), because 95% of the lung sites were treated without modulation (3DCRT and DCAT).

There were on average 2.6 CBCT acquisitions in SF SABR between 2010 and 2019, excluding POST CBCT. The most common scenario involved both 2 and 3 acquisitions (357 treatments each). Other common scenarios involved 1 and 4 acquisitions in 168 and 132 treatments, respectively. In 3 different treatments, 8, 10, and 12 CBCTs were acquired during a single session. No CBCT was acquired in 6 treatments due to exclusive use of the ExacTrac system.

The number of CBCTs acquired during a single session is shown in Figure 1d. The number of CBCT acquisitions was the largest in kidney site (number of CBCTs =  $3.5 \pm 1.4$ ,  $P$  values  $< 0.01$  for all comparisons between other sites). Midtreatment CBCTs were acquired in 559 treatments, where 36% (202 treatments) had a correction greater or equal to 2 mm in any direction.

### Parameters influencing treatment time in SF SABR

Treatment time was reduced through years, from a maximal treatment time of  $52 \pm 18$  min in 2012 to  $30 \pm 12$  min in 2019 ( $P$  value  $< 10^{-11}$ ). Small treatment times ( $< 20$  min) occurred when 2 sites were consecutively treated during same session. More than one site were treated during a single treatment session in 62 patients. Only one case involved 3 sites while all others involved 2 sites. In 70% of these patients, treatment times of subsequent treatments were shorter than the first treatment (median of subsequent treatment time over first treatment time = 0.85, interquartile range = 0.72-1.06). Large treatments time ( $> 60$  min) occurred in 35 treatments, involving either atypical long workflow (21 treatments), treatment interruption due to patient discomfort (10 treatments) or machine break-down (3 treatments), or repositioning after kV imaging (1 treatment), and needing further verification imaging. Percentage of treatments with duration larger than 60 min decreased from 22% (out of 9 treatments) in 2011 to 2% in 2019 (out of 221 treatments).

Figure 2a shows the treatment time for different treatment parameters. Treatment times were smaller with coplanar (CP) treatment compared with noncoplanar

(NCP) treatments ( $32 \pm 14$  min for CP and  $37 \pm 12$  min for NCP,  $P$  value  $< 10^{-9}$ ). Treatment times were reduced when using arc therapy (AT) compared with fixed gantry (FG) technique ( $31 \pm 13$  min for VMAT and DCAT combined and  $38 \pm 12$  min for 3DCRT and IMRT combined,  $P$  value  $< 10^{-12}$ ). The shortest mean treatment time was achieved with VMAT ( $29 \pm 14$  min) followed by DCAT ( $34 \pm 11$  min), 3DCRT ( $37 \pm 12$  min), and IMRT ( $40 \pm 13$  min). All differences between the treatment times per technique were statistically significant ( $P$  values ranged from  $10^{-15}$  to 0.02).

Treatment times per technique were dependent on the use of FFF as shown in Figure 2b. With FFF, the average treatment time for all techniques was  $28 \pm 11$  min compared with  $41 \pm 11$  min without FFF ( $P$  value  $< 10^{-12}$ ). There was a time reduction of 41%, 32%, 32%, 25%, when using FFF with VMAT, DCAT, IMRT, and 3DCRT, respectively (all  $P$  values  $< 10^{-5}$ ).

Treatment times per technique were further analyzed depending on the use of noncoplanar fields. Results are shown in Table 1. With FFF and coplanar treatment, the lowest treatment time was achieved with VMAT ( $24 \pm 9$  min,  $n = 145$ ; all  $P$  values  $< 10^{-2}$  in the comparison, except for DCAT treatment as all results for DCAT treatment were not statistically significant).

Treatment times per site based on the use of FFF are shown in Figure 2c. Using FFF reduced treatment time in all sites except soft tissues for which the difference between with flattening filter (WFF) and FFF was not statistically significant. Treatment times were reduced by 45% in vertebra, 38% in kidney, 31% in bone, 28% in lung, and 25% in node (all  $P$  values  $< 10^{-2}$  in comparing WFF with FFF for a given site). Treatment times per site, per technique, and FFF use are shown in Table 2. By considering only the sites for which more than 20 treatments had been delivered, the smallest mean treatment time was achieved in vertebra site by using VMAT, coplanar field and FFF ( $23 \pm 7$  min,  $n = 39$ ).

The treatment time and the prescription dose were very weakly correlated ( $\rho = 0.1$ ,  $P$  value  $< 10^{-5}$ ). A very weak correlation was also found between treatment time and MF ( $\rho = -0.1$ ,  $P$  value  $< 10^{-4}$ ). Furthermore, treatment time increased with the number of CBCTs acquired during a session ( $\rho = 0.5$ ,  $P$  value  $< 10^{-12}$ ) as shown in Figure 2d. The average time difference in the acquisition of a new CBCT was 6 min in considering 1 to 5 CBCT per session ( $P$  values  $< 10^{-3}$  for each comparison). Moreover, a moderate positive correlation between treatment time and number of CBCTs was observed for all sites ( $\rho$  ranged from 0.4-0.6 with  $P$  values  $< 10^{-4}$  for all correlations) except in SOFT site where the correlation was not statistically significant. Treatment time and number of CBCTs were correlated in all techniques, the correlation being positive and moderate in 3DCRT, VMAT, and IMRT treatments ( $\rho$  ranged from 0.5-0.6 with  $P$  values  $< 10^{-5}$  in all correlations) and positive and weak in DCAT

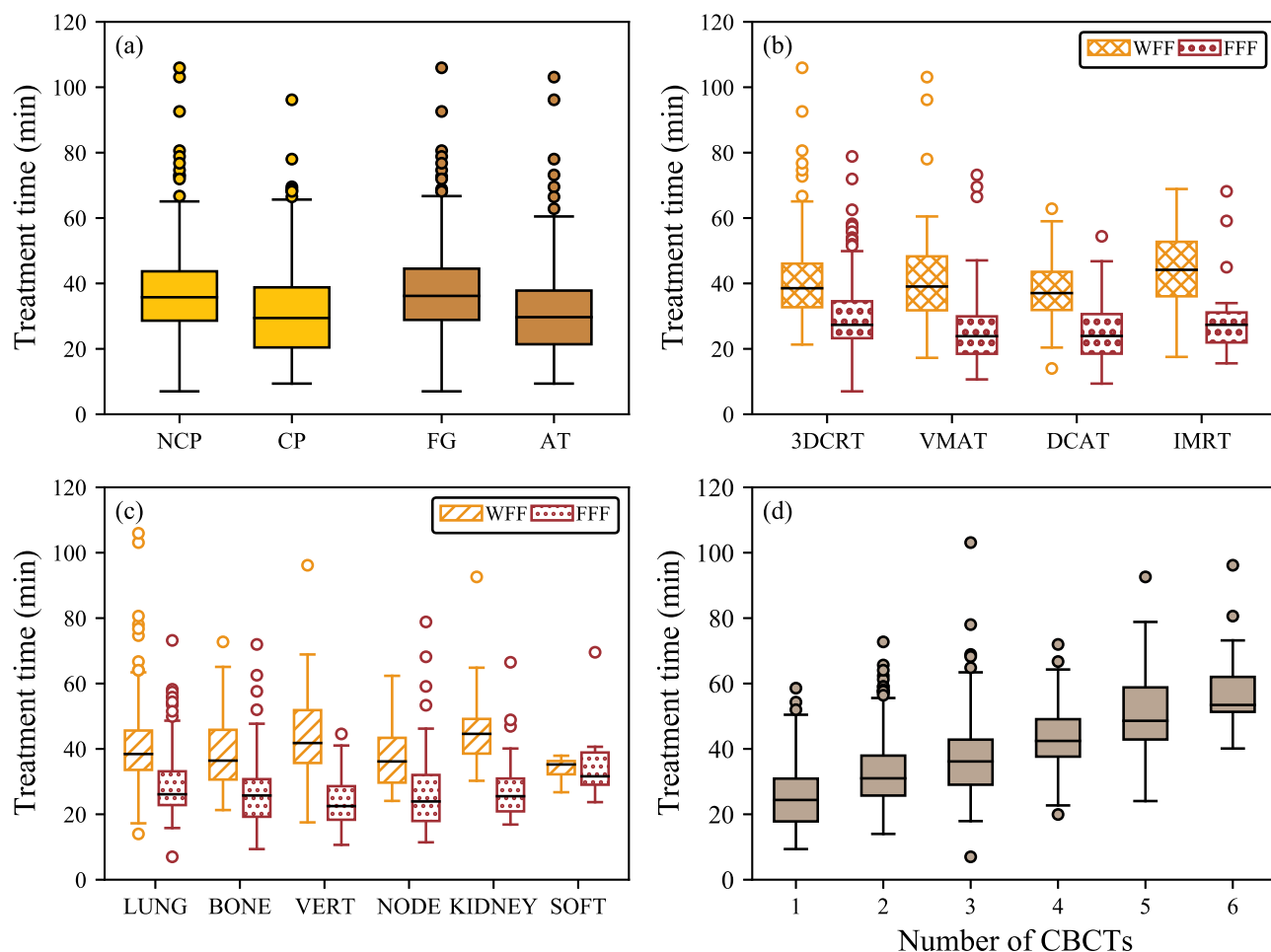


**Figure 2** (a) Comparison of the treatment time (min) between noncoplanar (NCP) and coplanar (CP) treatments and between fixed gantry (FG) and arc therapy (AT) treatments. Treatment time (min) per (b) technique and (c) site, depending on whether the dose rates were with flattening filter (WFF) or flattening filter free (FFF). (d) Treatment time (min) versus the number of cone beam computed tomographies (CBCT) acquired during a session.

treatment ( $\rho = 0.3$ ,  $P$  value  $< 10^{-4}$ ). The ExacTrac system was used in 224 treatments. Treatment times were reduced when using the ExacTrac system for VERT site (treatment time reduction of 30% and 20% in VMAT and IMRT respectively by using ExacTrac,  $P$  value  $< 10^{-2}$ ). However, no difference was observed in the treatment time for BONE site in 3DCRT treatment when using ExacTrac ( $P$  value = 0.64).

**Intrafraction correction in SF SABR**

The intrafraction correction across all treatments was  $1.7 \pm 1.6$  mm (95% of all treatments were  $< 4.6$  mm) as measured from MID-CBCT. Mean and standard deviations of the intrafraction correction during treatment for sites and techniques are shown in Table 3.

**Table 1** Treatment time (min) and the number of treatments for the different technique used, depending is FFF dose rate and noncoplanar field have been used

		Treatment time (mean $\pm$ standard deviation) in min (no. of treatments)			
		3DCRT	VMAT	DCAT	IMRT
FFF	Coplanar	33 $\pm$ 14 (11)	24 $\pm$ 9 (145)	24 $\pm$ 10 (30)	31 $\pm$ 15 (15)
	Noncoplanar	30 $\pm$ 11 (192)	32 $\pm$ 12 (22)	27 $\pm$ 8 (20)	26 $\pm$ 4 (7)
WFF	Coplanar	36 $\pm$ 10 (34)	42 $\pm$ 14 (42)	31 $\pm$ 6 (3)	44 $\pm$ 12 (54)
	Noncoplanar	41 $\pm$ 11 (381)	54 $\pm$ 36 (4)	38 $\pm$ 9 (104)	46 $\pm$ 9 (8)

*Abbreviations:* 3DCRT = 3-dimensional conformal radiotherapy; DCAT = dynamic conformal arc therapy; FFF = flattening filter free; IMRT = intensity modulated radiation therapy; WFF = with flattening filter; VMAT = volumetric modulated arc therapy.

**Table 2** Treatment time (mean  $\pm$  standard deviation) in minutes and number of treatments for all sites, depending if FFF or WFF was used and if the fields were coplanar (CP) or noncoplanar (NCP)

		Treatment time in min (no. of treatments) using FFF			
		3DCRT	VMAT	DCAT	IMRT
Lung	CP	30 $\pm$ 17 (3)	28 $\pm$ 8 (9)	26 $\pm$ 10 (17)	45 (1)
	NCP	29 $\pm$ 9 (142)	35 $\pm$ 19 (6)	29 $\pm$ 7 (14)	-
Bone	CP	31 $\pm$ 16 (6)	24 $\pm$ 8 (57)	23 $\pm$ 11 (8)	24 $\pm$ 6 (9)
	NCP	32 $\pm$ 13 (30)	30 $\pm$ 6 (7)	28 $\pm$ 8 (4)	29 $\pm$ 3 (2)
Vert	CP	-	23 $\pm$ 7 (39)	-	-
	NCP	32 (1)	41 (1)	-	27 (1)
Node	CP	44 (1)	21 $\pm$ 8 (17)	17 $\pm$ 8 (4)	52 $\pm$ 20 (3)
	NCP	35 $\pm$ 17 (13)	32 $\pm$ 12 (4)	15 $\pm$ 3 (2)	26 (1)
Kidney	CP	-	26 $\pm$ 12 (17)	36 (1)	28 $\pm$ 4 (2)
	NCP	40 $\pm$ 9 (5)	29 $\pm$ 5 (4)	-	21 $\pm$ 1 (2)
Soft	CP	41 (1)	37 $\pm$ 16 (6)	-	-
	NCP	31 (1)	-	-	32 (1)
		Treatment time in min (no. of treatments) using WFF			
		3DCRT	VMAT	DCAT	IMRT
Lung	CP	39 $\pm$ 13 (13)	43 $\pm$ 19 (7)	31 $\pm$ 6 (3)	-
	NCP	41 $\pm$ 10 (247)	54 $\pm$ 36 (4)	38 $\pm$ 9 (57)	47 (1)
Bone	CP	32 $\pm$ 5 (17)	44 $\pm$ 12 (8)	-	49 (1)
	NCP	39 $\pm$ 10 (84)	-	39 $\pm$ 10 (32)	53 (1)
Vert	CP	-	44 $\pm$ 16 (18)	-	44 $\pm$ 12 (52)
	NCP	32 (1)	-	-	45 $\pm$ 13 (4)
Node	CP	35 $\pm$ 8 (2)	36 $\pm$ 4 (3)	-	24 (1)
	NCP	42 $\pm$ 12 (9)	-	37 $\pm$ 8 (14)	-
Kidney	CP	45 $\pm$ 6 (2)	36 $\pm$ 7 (4)	-	-
	NCP	47 $\pm$ 12 (35)	-	-	45 $\pm$ 3 (2)
Soft	CP	-	35 $\pm$ 1 (2)	-	-
	NCP	32 $\pm$ 4 (5)	-	38 (1)	-

Abbreviations: 3DCRT = 3-dimensional conformal radiotherapy; DCAT = dynamic conformal arc therapy; FFF = flattening filter free; IMRT = intensity modulated radiation therapy; WFF = with flattening filter; VMAT = volumetric modulated arc therapy.

The correlations between intrafraction correction and treatment time and between the intrafraction correction and time to MID CBCT are shown in Table 4 for all sites and techniques. A positive and very weak correlation between treatment time and intrafraction correction magnitude was observed ( $\rho = 0.1$ ,  $P$  value = 0.03,  $n = 559$ ). Moreover, no correlation between intrafraction correction

magnitude and time to MID CBCT ( $P$  value = 0.75,  $n = 559$ ) was observed.

For treatments with corrections greater than 2 mm, a positive and weak correlation was observed between intrafraction variation magnitude and treatment time ( $\rho = 0.2$ ,  $P$  value  $< 10^{-2}$ ,  $n = 202$ ) and a positive and moderate correlation were observed between intrafraction variation

**Table 3** Intrafraction correction (mm) for sites and techniques measured from MID CBCT

MID CBCT					
Site	n	3D vector (mm)	Technique	n	3D vector (mm)
Lung	366	1.9 $\pm$ 1.6	3DCRT	401	1.7 $\pm$ 1.7
Bone	74	1.2 $\pm$ 1.6	VMAT	67	2.0 $\pm$ 1.9
Vert	33	0.8 $\pm$ 1.0	DCAT	58	1.4 $\pm$ 1.1
Node	28	1.3 $\pm$ 1.0	IMRT	33	0.9 $\pm$ 1.0
Kidney	44	1.4 $\pm$ 1.7			
Soft	14	2.1 $\pm$ 2.5			

Abbreviations: 3DCRT = 3-dimensional conformal radiotherapy; DCAT = dynamic conformal arc therapy; IMRT = intensity modulated radiation therapy; MID CBCT = mid-treatment cone-beam computed tomography; VMAT = volumetric modulated arc therapy.

**Table 4 Spearman's correlation coefficient ( $\rho$ ) and its associated  $P$  value between intrafraction variation magnitude and treatment time and between intrafraction variation magnitude and time between the start of the treatment and the MID CBCT (time to MID CBCT)**

Treatments	n	Treatment time		Time to MID CBCT	
		$\rho$	$P$ value	$\rho$	$P$ value
All	559	0.1*	0.03*	0.0	0.75
Lung	366	0.2*	< 10 <sup>-3</sup> *	0.0	0.54
Bone	74	0.1	0.35	0.1	0.34
Vert	33	-0.1	0.59	-0.1	0.57
Node	28	-0.1	0.58	-0.2	0.31
Kidney	44	0.1	0.56	0.0	0.93
Soft	14	0.2	0.52	0.2	0.53
3DCRT	401	0.1*	0.01*	0.0	0.90
VMAT	67	0.2	0.09	0.1	0.37
DCAT	58	0.2	0.10	0.0	0.85
IMRT	33	-0.3	0.12	-0.1	0.61

\* Significant results.  
 Abbreviations: 3DCRT = 3-dimensional conformal radiotherapy; DCAT = dynamic conformal arc therapy; IMRT = intensity modulated radiation therapy; MID CBCT = mid-treatment cone-beam computed tomography; VMAT = volumetric modulated arc therapy.

magnitude and total number of CBCTs ( $\rho = 0.5$ ,  $P$  value < 10<sup>-10</sup>,  $n = 202$ ). This is due to the institutional protocol of acquiring a second CBCT if the positional shift exceeds 2 mm in any direction.

## Discussion

Assuming equivalent safety and efficacy compared, single fraction SABR provides substantial efficiency gains compared with multifraction SABR regimes. This is particularly important in clinics with limited treatment time availability, when multiple targets require treatment, and when minimization of patient visits is beneficial.<sup>11,12</sup> In the present study, we have quantified the treatment duration for >1050 SF SABR treatments and determined treatment and image guidance factors that contribute to reduction in treatment time.

Treatment parameters that minimized treatment time were use of coplanar fields, arc therapy (VMAT or DCAT) and FFF dose rate, independently of the site treated. On average, FFF reduced treatment time by 13 minutes compared with WFF, arc therapy by 7 minutes compared with fixed gantry, and coplanar fields by 5 minutes compared with noncoplanar fields. The prescription dose and the modulation factor were not found to effect treatment time, which is dominated by imaging time over beam-on time. The most efficient treatment was achieved for vertebra sites through use of VMAT, coplanar arc therapy and FFF beams.

When more than one site were treated in the same session, treatment time of subsequent treatment was shorter than the first treatment time, a 0.85 time reduction in 50%

of these treatments in our data. This results is encouraging as more than one metastatic sites treated with SABR during the same session are currently investigated.<sup>3</sup>

As expected, increasing the number of CBCTs acquired in a treatment session increases the treatment session time; each CBCT added on average 6 minutes to the treatment time. This time interval includes the CBCT acquisition time, followed by matching and position correction. The use of planar orthogonal matching for bone and vertebral targets contributed to efficient treatment delivery compared with CBCT alone. In particular, if use of CBCTs can be reduced through use of during-treatment x-ray imaging such as fluoroscopy, or real-time intrafraction imaging, significant reductions in treatment time may be achieved, in addition to treatment geometric accuracy benefits.<sup>24–26</sup> For some patients, however, this may result in increased instances of target position variation during treatment being detected, which may require CBCT imaging to correct.

The intrafraction 3D positional shifts were <2 mm on average as measured from CBCT acquired during treatment for all sites. In the context of a GTV + 5 mm expansion margin (3 mm expansion for vertebra sites), our results for lung are in agreement with shift reported in the literature (between 1.3 and 1.7 mm).<sup>26,27</sup> Shifts for vertebra also agree with the literature (reported mean values between 0.5 and 0.7 mm).<sup>28,29</sup> Results for kidney are similar with previous results obtained by our group (1-1.3 mm).<sup>30</sup> Corrections for positional shifts were not correlated with the time between the beginning of the treatment and the MID CBCT acquisition. However, when the position shift based on midtreatment CBCT was larger than 2 mm in any direction, increased treatment time was positively correlated with increased 3D positional shift. According to our image guidance protocol, an additional CBCT is acquired when the positional correction exceeds 2 mm in any one direction (ie, <2 mm correction is applied when treated without repeating CBCT). Therefore, if a patient has a larger intrafraction variation, they will have increased imaging, which will in turn result in increased treatment time.

There are some limitations to the data extraction used in this investigation. Not all couch shift were recorded in the database due to system failure or online matching. Moreover, we were not able to extract midtreatment positional shifts for treatments in which the ExacTrac system was used.

On a different angle, a major component to treatment time reduction that cannot be measured with the database is the increase in efficiency and knowledge gained by the multidisciplinary team with time. In particular, the whole appointment time includes not only the image guidance and treatment, but initial patient setup. This depends on staff experience, immobilization equipment and patient compliance therefore may vary substantially between centers and patients.

Finally, SF SABR may benefit from magnetic resonance-guided radiation therapy, especially for lung, kidney, and liver site. This imaging technique provides superior determination of soft tissues compared with CT and real-time intrafraction visualization which may facilitate tumor tracking.<sup>31,32</sup> Note further that adaptive radiation therapy may be useful in SF SABR to account for variations in anatomy compared with that at time of treatment. In particular, adaptive radiation therapy may be useful where adjacent organs at risk are subject to frequent positional variation such as those in the abdomen or pelvis.<sup>31,33</sup>

## Conclusions

Use of single fraction SABR increased rapidly during the past decade. The optimal treatment parameters that minimized the treatment time were FFF dose rates, arc therapy (VMAT or DCAT), and coplanar arc for all sites. Furthermore, reducing the number of CBCTs acquired during a session led to a significant reduction in the treatment time. The intrafraction variation measured from the first CBCT acquired during delivery was  $1.7 \pm 1.6$  mm. Therefore, based on these results of set-up error, SF SABR treatment appears to be an attractive option to consider as a safe and efficacious treatment regime, in particular, when resources and patient visit are restricted.

## Acknowledgments

This work is funded in part by a Collaborative Research Agreement with Varian Medical Systems. This work is also funded in part by the Peter MacCallum Cancer Center Foundation. Shankar Siva is supported by the Victorian Cancer Council Colebatch Fellowship.

## References

- Benedict SH, Yenice KM, Followill D, et al. Stereotactic body radiation therapy: The report of AAPM Task Group 101. *Med Phys*. 2018;37:4078–4101.
- Foote M, Bailey M, Smith L, et al. Guidelines for safe practice of stereotactic body (ablative) radiation therapy. *J Med Imaging Radiat Oncol*. 2015;59:646–653.
- Palma DA, Olson R, Harrow S, et al. Stereotactic ablative radiotherapy for the comprehensive treatment of oligometastatic cancers: Long-term results of the SABR-COMET Phase II randomized trial. *J Clin Oncol*. 2020;38:2830–2837.
- Sogono P, Bressel M, David S, et al. Safety, efficacy, and patterns of failure after single-fraction stereotactic body radiation therapy (SBRT) for oligometastases. *Int J Radiat Oncol Biol Phys*. 2021;109:756–763.
- Aitken K, Hawkins M. Stereotactic body radiotherapy for liver metastases. *Clin Oncol*. 2015;27:307–315.
- Henderson DR, Tree AC, van As NJ. Stereotactic body radiotherapy for prostate cancer. *Clin Oncol*. 2015;27:270–279.
- Chang JH, Gandhidasan S, Finnigan R, et al. Stereotactic ablative body radiotherapy for the treatment of spinal oligometastases. *Clin Oncol*. 2017;29:E119–E125.
- Ball D, Mai G, Vinod S, et al. Stereotactic ablative radiotherapy versus standard radiotherapy in stage 1 non-small-cell lung cancer (TROG 09.02 CHISEL): A phase 3, open-label, randomised controlled trial. *Lancet Oncol*. 2019;20:494–503.
- Franks K, Jain P, Snee M. Stereotactic ablative body radiotherapy for lung cancer. *Clin Oncol*. 2015;27:280–289.
- Edvardsson A, Nordström F, Ceberg C, Ceberg S. Motion induced interplay effects for VMAT radiotherapy. *Phys Med Biol*. 2018;63:085012–085027.
- Faivre-Finn C, Fenwick JD, Franks KN, et al. Reduced fractionation in lung cancer patients treated with curative-intent radiotherapy during the COVID-19 pandemic. *Phys Med Biol*. 2020;32:481–489.
- Ng SSW, Ning MS, Lee P, McMahon RA, Siva S, Chuong MD. Single-fraction stereotactic body radiation therapy: A paradigm during the coronavirus disease 2019 (COVID-19) pandemic and beyond? *Adv Radiat Oncol*. 2020;5:761–773.
- Singh AK, Gomez-Suescun JA, Stephans KL, Bogart JA, Hermann GM, Tian L. One versus three fractions of stereotactic body radiation therapy for peripheral stage I to II non-small cell lung cancer: a randomized, multi-institution, phase 2 trial. *Int J Radiat Oncol Biol Phys*. 2019;105:752–759.
- Videtic GM, Hu C, Singh AK, Chang JY, Parker W, Olivier KR. A randomized phase 2 study comparing 2 stereotactic body radiation therapy schedules for medically inoperable patients with stage I peripheral non-small cell lung cancer: NRG Oncology RTOG 0915 (NCCTG N0927). *Int J Radiat Oncol Biol Phys*. 2015;93:757–764.
- Videtic GM, Paulus R, Singh AK, Chang JY, Parker W, Olivier KR. Long-term follow-up on NRG Oncology RTOG 0915 (NCCTG N0927): A randomized phase 2 study comparing 2 stereotactic body radiation therapy schedules for medically inoperable patients with stage I peripheral non-small cell lung cancer. *Int J Radiat Oncol Biol Phys*. 2019;103:1077–1084.
- Gandhidasan S, Ball D, Kron T, et al. Single fraction stereotactic ablative body radiotherapy for oligometastasis: Outcomes from 132 consecutive patients. *Clin Oncol*. 2018;30:178–184.
- Huo M, Sahgal A, Pryor D, Redmond K, Lo S, Foote M. Stereotactic spine radiosurgery: Review of safety and efficacy with respect to dose and fractionation. *Surg Neurol Int*. 2017;8.
- Kang Zeng L, Tseng CL, Soliman H, Weiss Y, Sahgal A. Stereotactic body radiotherapy (SBRT) for oligometastatic spine metastases: An overview. *Front Oncol*. 2019;9:1–11.
- Pham D, Thompson A, Kron T, et al. Stereotactic ablative body radiation therapy for primary kidney cancer: A 3-dimensional conformal technique associated with low rates of early toxicity. *Int J Radiation Oncol Biol Phys*. 2014;90:1061–1068.
- Senger C, Conti A, Klude A, et al. Robotic stereotactic ablative radiotherapy for renal cell carcinoma in patients with impaired renal function. *BMC Urol*. 2019;19:96–105.
- Ong CL, Dahele M, Slotman BJ, Wilko FARV. Dosimetric impact of the interplay effect during stereotactic lung radiation therapy delivery using flattening filter-free beams and volumetric modulated arc therapy. *Int J Radiation Oncol Biol Phys*. 2013;86:743–748.
- Gauer T, Sothmann T, Blanck O, Petersen C, Werner R. Underreported dosimetry errors due to interplay effects during VMAT dose delivery in extreme hypofractionated stereotactic radiotherapy. *Strahlenther Onkol*. 2018;194:570–579.
- Siva S, Devereux T, Kron T, et al. Vacuum immobilisation reduces tumour excursion and minimises intrafraction error in a cohort study of stereotactic ablative body radiotherapy for pulmonary metastases. *J Med Imaging Radiat Oncol*. 2014;58:244–252.
- Keall P, Trang Nguyen D, O'Brien R, et al. Real-time image guided ablative prostate cancer radiation therapy: Results from the TROG 15.01 SPARK trial. *Int J Radiat Oncol Biol Phys*. 2020;107:530–538.

25. Kim JH, Nguyen DT, Booth JT, et al. The accuracy and precision of Kilovoltage Intrafraction Monitoring (KIM) six degree-of-freedom prostate motion measurements during patient treatments. *Radiother Oncol.* 2018;126:236–243.
26. Hazelaar C, Verbakel WFAR, Mostafavi H, van der Weide L, Slotman BJ, Dahele M. First experience with markerless online 3D spine position monitoring during SBRT delivery using a conventional LINAC. *Int J Radiat Oncol Biol Phys.* 2018;101:1253–1258.
27. Bissonnette JP, Franks KN, Purdie TG, et al. Quantifying interfraction and intrafraction tumor motion in lung stereotactic body radiotherapy using respiration-correlated cone beam computed tomography. *Int J Radiat Oncol Biol Phys.* 2009;75:688–695.
28. Hyde D, Lochray F, Korol R, et al. Spine stereotactic body radiotherapy utilizing cone-beam CT image-guidance with a robotic couch: Intrafraction motion analysis accounting for all six degrees of freedom. *Int J Radiat Oncol Biol Phys.* 2012;82:e555–e562.
29. Rossi E, Fiorino C, Fodor A, et al. Residual intra-fraction error in robotic spinal stereotactic body radiotherapy without immobilization devices. *Phys Imaging Radiat Oncol.* 2020;16:20–25.
30. Pham D, Kron T, Bressel M, et al. Image guidance and stabilization for stereotactic ablative body radiation therapy (SABR) treatment of primary kidney cancer. *Practical Radiation Oncology.* 2015;5:e597–e605.
31. Finazzi T, van Sörnsen de Koste JR, Palacios MA, et al. Delivery of magnetic resonance-guided single-fraction stereotactic lung radiotherapy. *Phys Imaging Radiat Oncol.* 2020;14:17–20.
32. Kron T, Thorwarth D. Single-fraction magnetic resonance guided stereotactic radiotherapy: A game changer? *Phys Imaging Radiat Oncol.* 2020;14:95–96.
33. Tetar SU, Bohoudi O, Senan S, et al. The role of daily adaptive stereotactic MR-guided radiotherapy for renal cell cancer. *Cancers.* 2020;2774:2763.